

Published in final edited form as:

*Cancer Res.* 2015 January 1; 75(1): 111–119. doi:10.1158/0008-5472.CAN-14-2040.

## LASP1 is a HIF-1 $\alpha$ target gene critical for metastasis of pancreatic cancer

Tiansuo Zhao<sup>1, #</sup>, He Ren<sup>1, #</sup>, Jing Li<sup>1, #</sup>, Jing Chen<sup>1</sup>, Huan Zhang<sup>1</sup>, Wen Xin<sup>1</sup>, Yan Sun<sup>1</sup>, Lei Sun<sup>1</sup>, Yongwei Yang<sup>1</sup>, Junwei Sun<sup>1</sup>, Xiuchao Wang<sup>1</sup>, Song Gao<sup>1</sup>, Chongbiao Huang<sup>1</sup>, Huafeng Zhang<sup>2</sup>, Shengyu Yang<sup>3</sup>, and Jihui Hao<sup>1, \*</sup>

<sup>1</sup>Tianjin Medical University Cancer Institute and Hospital, National Clinical Research Center for Cancer; Key Laboratory of Cancer Prevention and Therapy, Department of Pancreatic Cancer, Tianjin, 300060, China

<sup>2</sup>School of Life Science, University of Science and Technology of China, Hefei, Anhui, 230027, China

<sup>3</sup>Department of Tumor Biology and Comprehensive Melanoma Research Center, H. Lee Moffitt Cancer Center & Research Institute, Tampa, FL 33612

### Abstract

LASP1 is an actin-binding protein associated with actin assembly dynamics in cancer cells. Here we report that LASP1 is overexpressed in pancreatic ductal adenocarcinoma (PDAC) where it promotes invasion and metastasis. We found that LASP1 overexpression in PDAC cells was mediated by HIF-1 $\alpha$  through direct binding to a hypoxia response element in the LASP1 promoter. HIF-1 $\alpha$  stimulated LASP1 expression in PDAC cells in vitro and mouse tumor xenografts in vivo. Clinically, LASP1 overexpression in PDAC patient specimens was associated significantly with lymph node metastasis and overall survival. Overall, our results defined LASP1 as a direct target gene for HIF-1 $\alpha$  upregulation that is critical for metastatic progression of PDAC.

### Keywords

Pancreatic ductal adenocarcinoma; Hypoxia-inducible factor-1 $\alpha$ ; LASP-1; Metastasis

### Introduction

Despite recent advances in the diagnosis and therapeutic modalities, pancreatic ductal adenocarcinoma (PDAC) remains the digestive-tract tumor with the poorest prognosis (1). PDAC is the fourth highest cause of cancer-related deaths in the United States, with a 5-year survival rate lower than 5% (2). The aggressive course of PDAC progression is mostly due to delayed diagnosis, resistance to conventional chemotherapies and development of

\*Correspondence should be addressed to: Jihui Hao, Department of Pancreatic Cancer, Tianjin Medical University Cancer Institute and Hospital, Tianjin 300060, China. Telephone: +86-022-23340123; haojihui@tjmuch.com.

#The first three authors contributed equally to this work.

### Conflict of interest statement

No potential conflicts of interest were disclosed.

metastasis (3). The underlying mechanisms that trigger PDAC invasion and metastasis remained largely unknown, although it is believed that the hypoxic microenvironment and hypoxia-induced factors are critical drivers of PDAC metastasis and progression (4).

LIM and SH3 protein 1 (LASP-1) is an actin-binding protein containing an N-terminal LIM domain and two actin-binding domains in the core of LASP-1 protein (5). LASP-1 was first identified from a cDNA library of metastatic axillary lymph nodes of breast cancer patients, and the gene was mapped to human chromosome 17q21 (6, 7). LASP-1 interacts with the actin cytoskeleton at the site of cell membrane extensions, but not along actin stress fibers (5, 8–10). The SH3 domain at the C-terminus is involved in interactions with zyxin, pallidin, lipoma-preferred partner, and vasodilator-stimulated phosphoprotein (9, 11). LASP-1 reportedly localizes within multiple sites of dynamic actin assembly, such as focal contacts, focal adhesions, lamellipodia, membrane ruffles, and pseudopodia, and is involved in cell proliferation and migration (12). It was previously reported that LASP-1 overexpression induced cell proliferation and migration in human breast cancer, ovarian cancer, colorectal cancer, malignant childhood medulloblastoma, and hepatocellular carcinoma (5, 13–16). However, the role of LASP-1 in PDAC progression has not been examined.

In this study, we aim to investigate the role of LASP-1 in PDAC progression. Our data showed that LASP-1 was overexpressed in PDAC, and LASP-1 overexpression promoted PDAC cell migration and invasion *in vitro* and metastasis in xenograft mouse models. LASP-1 overexpression in PDAC is mediated by HIF-1 $\alpha$ , which directly binds to and transactivates the LASP-1 promoter. Our findings indicate that LASP-1 is a novel direct HIF-1 $\alpha$  target gene that promotes PDAC metastasis and progression.

## Materials and methods

### Cell culture and hypoxic treatment

Human PDAC cell lines, CFPAC-1, BxPC-3 and Panc-1 were obtained from the Committee of Type Culture Collection of Chinese Academy of Sciences (Shanghai, China) and MIA-PaCa-2 was obtained from the American Type Culture Collection. All the cell lines were obtained in 2013, and recently authenticated in August 2014 through the short tandem repeat analysis method. These cells were grown at 37 °C in a humidified atmosphere of 95% air and 5% CO<sub>2</sub> using Dulbecco's modified Eagle medium (DMEM) with 10% fetal bovine serum (FBS). For hypoxic treatment, cells were placed in a modulator incubator (Thermo Electron Co., Forma, MA, USA) in an atmosphere consisting of 93.5% N<sub>2</sub>, 5% CO<sub>2</sub>, and 1.5% O<sub>2</sub>.

### Western blot analysis

Whole-cell extracts were prepared by lysing cells with RIPA lysis buffer supplemented with a proteinase inhibitor cocktail (Sigma). Protein concentrations were quantified using Pierce protein assay kit (Pierce). Protein lysates (20  $\mu$ g) were separated by SDS-PAGE, and target proteins were detected by Western blot analysis with antibodies against HIF-1 $\alpha$  (1:1000), LASP-1 (1:2000), and  $\beta$ -actin (1:1000) (Table S1). Specific proteins were visualized using an enhanced chemiluminescence detection reagent (Pierce).

### Reverse-transcription polymerase chain reaction (RT-PCR)

Total RNA was isolated from transfected cells with TRIzol Reagent (Invitrogen) and used for first-strand cDNA synthesis using the First-Strand Synthesis System for RT-PCR (Takara). Each sample was processed in triplicate, and  $\beta$ -actin was used as loading control. Each experiment was repeated independently for at least three times. PCR primers used are indicated in Table S1.

### Immunofluorescence

To assess LASP-1 and F-actin distribution, human PDAC cells were seeded onto glass slides for different treatments. The cells were then washed once with PBS and fixed with 4% paraformaldehyde in PBS for 15 min, permeabilized with 0.1% Triton X-100 in PBS for 30 min at room temperature, and blocked for 1 h with 3% BSA in PBS. Then cells were stained with anti-LASP-1 antibody (1:200 dilution, overnight at 4 °C). F-actin was stained with phalloidin-FITC (Beyotime Biotechnology). Cells were mounted with DAPI Fluoromount-G media with DAPI nuclear stain (Southern Biotech). Slides were viewed with Olympus confocal microscopy.

### Chromatin immunoprecipitation assay

Chromatin immunoprecipitation assay was performed using a commercial kit (Upstate Biotechnology) according to the manufacturer's instructions. Primers flanking the hypoxia response elements (HREs) of the VEGF promoter were used as a positive control (17, 18). The PCR primers are indicated in Table S1.

### siRNA duplexes, plasmid constructs, transient transfection, stable transfection in pancreatic cancer cells and luciferase assay

Small interfering RNAs (siRNAs) against LASP-1 and HIF-1 $\alpha$  were designed and synthesized from GenePharma (Shanghai, China) (Table S1). The human LASP-1 cDNA was cloned into the pcDNA3.1 plasmid expression vector. The pcDNA3.1-HIF-1 $\alpha$  plasmids were prepared as previously described (17, 18).

LASP-1 overexpression in Panc-1 cells, Lentivirus-mediated plasmid was done using the pLV-cDNA system (Biosettia) following the manufacturer's instructions. Lentivirus encoding DNA were packaged as previously described (19). Following transfection, the medium containing Lentivirus was collected, filtered, and transferred onto Panc-1 cells. Infected cells were selected with puromycin (1 $\mu$ g/mL) for 7 days.

Genomic DNA fragments of the human LASP1 gene, spanning from +1 to -2000 relative to the transcription initiation sites were generated by PCR and inserted into pGL3-Basic vectors (denoted as pGL3-LASP-1). All constructs were sequenced to confirm their identity. Luciferase activity was measured using the Dual-Luciferase Reporter Assay System (Promega) as previously described (17, 18). For transfection, cells were plated at a density of  $5 \times 10^5$  cells/well in 6-well plates with serum-containing medium. When the cells were 80% confluent, the siRNA duplexes or overexpression plasmids were transfected into cells using Lipofectamine-2000 (Invitrogen) for 48 h. The cells were collected for cell migration and invasion analysis, western blot analysis, and RT-PCR, immunofluorescence, etc.

### Wound healing and Cell migration assay

A wound healing assay was performed according to published protocol (20). Invasion assays were performed with 8.0 $\mu$ m pore inserts in a 24-well Trans-well. For this assay,  $1 \times 10^5$  cells were isolated and added to the upper chamber of a trans-well with DMEM. The invasion assay was performed using 1/6 diluted matrigel (BD Bioscience)-coated filters. DMEM with 10% fetal bovine serum was added to the lower chamber and the cells were allowed to incubate for 24 hours. Cells that had migrated to the bottom of the filter were stained with a three-step stain set (Thermo Scientific). All experiments were repeated independently for at least three times.

### Animal studies and measurement of metastasis in orthotopic pancreatic cancer mouse model

Female 4-week-old nude nu/nu mice were maintained in a barrier facility on HEPA-filtered racks. All animal studies were conducted under an approved protocol in accordance with the principles and procedures outlined in the NIH Guide for the Care and Use of Laboratory Animals. Digoxin and saline for injection were obtained from Tianjin Medical University Cancer Institute and Hospital. Cells were harvested by trypsinization, washed in PBS, resuspended at  $10^7$  cells/ml in a 1:1 solution of PBS/Matrigel, and injected subcutaneously into the right flank of 16 nude nu/nu mice. Primary tumors were measured in 3 dimensions (a, b, c), and volume was calculated as  $abc \times 0.52$  (21). Primary tumors were harvested from the flank of nude nu/nu mice. Part of the tumor was fixated by formalin and embedded using paraffin, and the rest of the tumor was used for protein extraction.

For orthotopic tumor cell injection, 18 nude nu/nu mice were divided into three groups (Panc-1/pLV Vector+saline, Panc-1/pLV Vector+digoxin and Panc-1/pLV LASP-1+digoxin, respectively, 6 mice each).  $2.0 \times 10^6$  cells were injected into the carefully exposed pancreas of nude mice. The pancreas was then returned to the peritoneal cavity; the abdominal wall, and the skin was closed with skin clips. Six weeks later, the number of visible metastatic lesions in the gut, mesentery and liver was determined (22).

### Immunohistochemistry

With approval from the Ethics Committee, PDAC samples were obtained from 91 patients (aged 36 years to 83 years) undergoing surgical resection with histologic diagnosis of PDAC at the Tianjin Cancer Institute and Hospital. Immunohistochemistry for HIF-1 $\alpha$  and LASP-1 of PDAC patient tissues was performed using a DAB substrate kit (Maxin, Fuzhou, China). Immunoreactivity was semiquantitatively scored according to the estimated percentage of positive tumor cells as previously described (18). Staining intensity was scored 0 (negative), 1 (low), 2 (medium), and 3 (high). Staining extent was scored 0 (0% stained), 1 (1%–25% stained), 2 (26%–50% stained), and 3 (51%–100% stained). The final score was determined by multiplying the intensity scores with staining extent and ranged from 0 to 9. Final scores (intensity score  $\times$  percentage score) less than 2 were considered as negative staining (–), 2–3 were low staining (+), 4–6 were medium staining (++) and  $>6$  were high staining (+++).

## Statistical analysis

Student's *t*-test for paired data was used to compare mean values. ANOVA is used to analysis two groups' data with continuous variables. Non-parametric data were analyzed with Mann-Whitney U test. The categorical data was analyzed by either Fisher's exact or Chi-Square method. Each experiment was conducted independently for at least three times, and values were presented as mean  $\pm$  standard deviation (SD), unless otherwise stated. Analyses were performed using SPSS18.0 statistical analysis software.

## Results

### LASP-1 overexpression promoted PDAC cell migration and invasion

To determine the role of LASP-1 in PDAC progression, we compared its expression levels in PDAC specimens and paired adjacent normal pancreatic tissues from PDAC patients. Despite inter-individual variations, LASP-1 protein (Figure 1A) and mRNA (Figure 1B) levels were found to be evidently upregulated in PDAC samples when compared to adjacent normal pancreatic tissues, suggesting that LASP-1 was activated at transcriptional levels during PDAC progression. Furthermore, LASP-1 signal measurement by immunohistochemistry was detected in most (87.9%) of PDAC tissues (Figure 1C). Intriguingly, in pancreas tumors other than malignant PDAC, such as benign tumors: serous cystadenoma and neuroendocrine tumor, LASP-1 expression was negative (Figure 1C).

Next we set out to examine the effects of LASP-1 overexpression on PDAC cell migration and invasion. To investigate the role of LASP-1 in the aggressive phenotypes of PDAC cells *in vitro*, we used siRNA transfection to knockdown LASP-1 expression in two PDAC cell lines with high endogenous LASP-1 levels (CFPAC-1 and MIA-PaCa-2) (Figure 2A). Out of the three pairs of siRNA, siRNA #3 most efficiently knockdown LASP-1 expression by more than 70% (Figure 2B, C), and was used in the subsequent functional studies. Cell migration and invasion analysis using transwell assay suggested that LASP-1 depletion in CFPAC-1 and MIA-PaCa-2 cells evidently reduced cell migration and invasion (Figure 2D). In the wound-healing assays, the migratory activity of CFPAC-1 and MIA-PaCa-2 cells was also inhibited by LASP-1 silencing (Figure 2E). Immunofluorescence analysis confirmed regional co-localization between LASP-1 and F-actin (Figure 2F). Interestingly, compared with CFPAC-1/siNC and MIA-PaCa-2/siNC cells, the morphology of CFPAC-1/siLASP-1 and MIA-PaCa-2/siLASP-1 cells lacked thin and long pseudopods (Figure 2F). These data indicated that LASP-1 was critical for the migration and invasion of PDAC cells.

To determine whether LASP-1 overexpression is sufficient to promote PDAC cell migration, LASP-1 was ectopically expressed in two PDAC cell lines with low endogenous LASP-1 levels (BxPC-3 and Panc-1) (Figure S1). Cell migration and invasion analysis by transwell assay suggested that LASP-1 upregulation in BxPC-3 and Panc-1 cells evidently increased cell migration and invasion (Figure 2G). Wound-healing assays showed that the migratory activity of the BxPC-3 and Panc-1 cells was enhanced by LASP-1 overexpression when compared with the control cells (Figure 2H). Importantly, BxPC-3/pcDNA3.1-LASP1 and Panc-1/pcDNA3.1-LASP1 displayed some pseudopods extending from cell bodies

(Figure 2I). These results showed that ectopic overexpression of LASP-1 was sufficient to promote PDAC cell migration and invasion.

### **HIF-1 $\alpha$ directly regulated the expression of LASP-1 through binding to the HRE in the LASP-1 gene promoter**

Our previous study indicated HIF-1 as a critical transcriptional factor in pancreatic cancer cell migration (18, 23). To determine whether HIF-1 regulates transcription of LASP-1 in pancreatic cancer cells, we used specific siRNAs targeting HIF-1 $\alpha$  to effectively reduce HIF-1 $\alpha$  expression (Figure S2). Knockdown of HIF-1 $\alpha$  expression decreased LASP-1 mRNA (Figure 3A, left) and protein (Figure 3A, right) expression ( $p<0.05$ ). Moreover, when HIF-1 $\alpha$  was overexpressed in Panc-1 cells, LASP-1 mRNA (Figure 3B, left) and protein (Figure 3B, right) expression markedly increased ( $p<0.05$ ). Taken together, these results suggest that HIF-1 $\alpha$  plays a critical role in LASP-1 expression.

To determine whether hypoxia may induce LASP-1 overexpression in PDAC cells, four PDAC cell lines were cultured under normoxia (21% O<sub>2</sub>) and hypoxia (1.5% O<sub>2</sub>) for 12 hours and the LASP-1 expression levels were determined by western blot analysis. As shown in Figure 3C, LASP-1 expression increased about 3.85 fold after hypoxic treatment when compared with normoxia cultured cells, suggesting that hypoxic PDAC microenvironment might be responsible for LASP-1 overexpression.

To understand the molecular mechanism underlying LASP-1 overexpression in PDAC, we survey the promoter region of human LASP-1 gene and identified 4 hypoxia response elements (HREs) (Figure 3D).

To investigate whether HIF-1 $\alpha$  directly binds to LASP-1 promoter, chromatin immunoprecipitation assay was performed in Panc-1 cells at 1.5% O<sub>2</sub> or 21% O<sub>2</sub>. In chromatin fractions pulled down by an anti-HIF-1 $\alpha$  antibody, only the HRE of LASP-1 promoter located at -1005 to -1001 was detected (Figure 3E, upper). The fragment immunoprecipitated by anti-HIF-1 $\alpha$  antibody significantly increased (Figure 3E, lower,  $p<0.01$ ) under hypoxia, suggesting that hypoxia promoted the binding of HIF-1 $\alpha$  to LASP-1 promoter.

To determine whether the binding of HIF-1 $\alpha$  activates LASP-1 promoter, we constructed a full-length LASP-1 luciferase promoter vector (containing HREs, -1005 to -1001) and co-transfected this reporter construct with or without HIF-1 $\alpha$  cDNA into Panc-1 cells. Luciferase analysis showed that HIF-1 $\alpha$  overexpression (pcDNA-HIF1 $\alpha$ ) significantly increased LASP-1 promoter activity in Panc-1 cells (~2.9-fold,  $p<0.05$ ) (Figure 3F). To determine whether the HRE1 site is required for HIF-1 $\alpha$  to transactivate LASP-1 promoter, this HIF-1  $\alpha$  binding site was mutated from ACGTG to ACATG. As shown in Figure 3F, the mutation of HRE1 almost abolished the transactivation of LASP-1 promoter by HIF-1 $\alpha$ . (VEGF promoter was used as the positive control).

### **HIF-1 $\alpha$ upregulates LASP-1 expression in xenograft mouse model**

To determine whether HIF-1 $\alpha$  regulates LASP-1 expression in vivo, we injected Panc-1 cells subcutaneously into the right flank of nude nu/nu mice. When the tumors reached 100

mm<sup>3</sup>, the mice were i.p. injected with saline or digoxin (2 mg/kg) on daily basis to inhibit HIF activity (21, 24, 25). The tumor was palpable at 5 days after inoculation and that all of the mice had developed tumors by the end of the experiment. Compared with saline control group, the average tumor volume in digoxin group was reduced obviously ( $p<0.01$ ) (Figure 4A, B and C). Next, we evaluated the association between HIF-1 $\alpha$  and LASP-1 by Western blot (Figure 4D) and immunohistochemistry (Figure 4E) and the results suggest that expression of LASP-1 was decreased as a result of the HIF-1 $\alpha$  level reduction by digoxin.

### **HIF-1 correlates with LASP-1 expression in the specimens of human PDAC**

To determine whether HIF-1 indeed regulates the expression of LASP-1 in PDAC patients, we performed immunohistochemical staining to determine HIF-1 $\alpha$  and LASP-1 levels in PDAC specimens. As shown in Figure 4F, LASP-1 expression co-localized with HIF-1 $\alpha$  in consecutive sections of PDAC tissues at different grades. Importantly, HIF-1 $\alpha$  expression in PDAC specimens significantly correlated with the levels of LASP-1 (Figure 4G and 4H), implicating that HIF-1 $\alpha$  is a critical regulator for LASP-1 overexpression in PDAC patients.

### **LASP-1 overexpression is able to rescue the inhibition of PDAC metastasis by HIF-1 knockdown**

To understand the role of LASP-1 in HIF-1 $\alpha$ -mediated migration, we ectopically expressed LASP-1 in HIF-1 $\alpha$  knockdown Panc-1 and CFPAC-1 cells. As shown in Figures 5A (Panc-1: left; CFPAC-1: right), LASP-1 overexpression at least partially rescued the inhibitory effect of HIF-1 $\alpha$  knockdown on PDAC cell migration ( $p<0.05$ ), suggesting that LASP-1 was involved in HIF-1 $\alpha$ -mediated migration.

To confirm the role for LASP-1 in pancreatic cancer cell invasion and metastasis in vivo, we developed an orthotopic pancreatic cancer mouse model using Panc-1/pLV Vector and Panc-1/pLV LASP-1 cells. When compared with Panc-1/pLV Vector cells, the morphology of Panc-1/pLV LASP-1 cells became irregular and have the thin and long pseudopods (Figure S3A). The up-regulation of LASP-1 protein in Panc-1/pLV LASP-1 cells was confirmed by western blot experiment (Figure S3B). When injected orthotopically, Panc-1 cells developed primary tumor in the pancreas and distant metastases in the liver, gut and mesentery over the course of 6 weeks. The size of primary pancreatic tumor and metastases of liver, gut and mesentery in Panc-1/pLV Vector group was suppressed by digoxin treatment (mean  $\pm$  SD: 9.17 $\pm$ 1.47) versus (3.33 $\pm$ 1.03,  $p<0.01$ ) (Figure 5B, C). However, the Panc-1/pLV LASP-1+digoxin group developed a significantly larger primary pancreatic tumor and higher number of metastatic lesions in liver, gut and mesentery when compared with Panc-1/pLV Vector+digoxin tumors (mean  $\pm$  SD: 3.33 $\pm$ 1.03) versus (22.83 $\pm$ 2.79,  $p<0.01$ ) (Figure 5B, C). The tumors from pancreas, liver, gut and spleen were further confirmed by hematoxylin-eosin staining (Figure 5D). Taken together, these results suggested that overexpression of LASP-1 is critical for HIF-1 $\alpha$  mediated PDAC metastasis.

### **LASP-1 correlated with lymph node metastasis in PDAC patients**

Our in vitro data suggest that LASP-1 overexpression may contribute to PDAC progression by promoting PDAC cell migration, invasion and metastasis. To further critically examine this possibility, we evaluate the correlation between LASP-1 expression levels and

clinicopathological features and overall survival among our cohort of PDAC patients (Table 1). There was no obvious correlation between expression of LASP-1 and age, gender and histological grade of PDAC patients. However, LASP-1 expression was correlated with the pathological tumor node metastasis stage ( $\chi^2=21.806$ ,  $p<0.05$ ) and lymph node metastasis ( $\chi^2=17.481$ ,  $p<0.01$ ) of PDAC samples (Table 1). Importantly, PDAC patients with high or medium (+++or++) LASP-1 protein expression had significantly worse overall survival than those with negative or low (-or+) LASP-1 expression ( $p=0.008$ ) (median time, 8 and 16 months) (Figure 6). Taken together, these data indicated that LASP-1 correlates with lymph node metastasis and influences the prognosis of PDAC patients.

## Discussion

In this study, we investigated the role of LASP-1 in PDAC progression and metastasis. Our data showed that LASP-1 expression levels were higher in PDAC than in adjacent non-tumorous tissues. Intriguingly, LASP-1 overexpression was also observed in metastatic breast (13), ovarian (14), colorectal (15), and hepatocellular cancer (26) tissues and cell lines. Our mechanistic studies revealed that LASP-1 overexpression in PDAC was mainly mediated by HIF-1 $\alpha$ , which directly binds to a hypoxia response element on LASP-1 promoter. Importantly, HIF-1 $\alpha$  inhibition with digoxin drastically reduced LASP-1 protein levels in a PDAC xenograft mouse model. Moreover, IHC staining on consecutive sections of PDAC specimens indicated strong correlation between HIF-1 $\alpha$  levels and LASP-1 levels. These observations strongly support LASP-1 as a novel direct target gene of HIF-1 $\alpha$  in PDAC.

Hypoxia is commonly presented in the microenvironment of solid tumors (27). The constitutive expression of HIF-1 $\alpha$  in PDAC was also previously reported (28). Our data indicated that elevated HIF-1 $\alpha$  levels in PDAC transactivates LASP-1 gene transcription and protein expression, which in turn dysregulate the actin cytoskeleton in metastatic PDAC cells to promote invasion and metastasis. Intriguingly, HIF-1 $\alpha$  also transactivate the gene transcription of the pro-metastasis actin-bundling protein fascin-1 (23). Taken together, these findings indicated that HIF-1 $\alpha$  is a key regulator of the actin network remodeling in during cancer invasion and metastasis. By up-regulating LASP-1 and fascin-1, HIF-1 $\alpha$  promotes the formation of membrane protrusions such as lamellipodia and filopodia, which provides driving forces for PDAC cell motility, invasiveness and dissemination (29–32). In addition to the HIF-1/LASP-1 signaling pathway, other pathways such as TGF- $\beta$  (33), SLIT2-ROBO (34) and CXCL12/CXCR4 (35) signaling pathways, also influence PDAC metastasis. Understanding the interaction among these pathways may provide new clues for inhibiting metastasis of PDAC.

Our data indicated that LASP-1 might play a causal role in PDAC metastasis. Indeed, LASP-1 expression in PDAC patients strongly associated with lymph node metastasis and poor clinical prognosis. Furthermore, we showed that LASP-1 indeed promoted the liver, gut and mesentery metastases by using the orthotopic xenograft mouse model of pancreatic cancer. In summary, results from in vitro and in vivo experiments indicated that LASP-1 overexpression was a critical driver for PDAC cell migration and metastasis.



In summary, we demonstrated that LASP-1 was upregulated in PDAC particularly in those with metastasis, thereby indicating its relationship with poor clinical prognosis. LASP-1 stimulated cancer cell metastasis and aggressive phenotypes *in vitro* and *in vivo*. Most importantly, HIF-1 $\alpha$  regulated LASP-1 expression by binding to the HRE. Therefore, inhibiting LASP-1 expression may be more effective for treating metastatic PDAC.

## Supplementary Material

Refer to Web version on PubMed Central for supplementary material.

## Acknowledgments

National Natural Science Foundation of China (Grant No. 81302082, 81272685, 31301151, 81172355, 31471340, 31470957, 81472264, 81401957); Key Program of Natural Science Foundation of Tianjin (Grant No. 11JCZDJC18400, 13YCYBYC37400); Major Anticancer Technologies R & D Program of Tianjin (Grant No. 12ZCDZSY16700). S. Yang is supported by NIH (R01CA175741).

## References

1. Tan CR, Yaffee PM, Jamil LH, Lo SK, Nissen N, Pandol SJ, et al. Pancreatic cancer cachexia: a review of mechanisms and therapeutics. *Frontiers in physiology*. 2014; 5:88. [PubMed: 24624094]
2. Siegel R, Ma J, Zou Z, Jemal A. Cancer statistics, 2014. *CA Cancer J Clin*. 2014; 64:9–29. [PubMed: 24399786]
3. Vincent A, Herman J, Schulick R, Hruban RH, Goggins M. Pancreatic cancer. *Lancet*. 2011; 378:607–20. [PubMed: 21620466]
4. Spivak-Kroizman TR, Hostetter G, Posner R, Aziz M, Hu C, Demeure MJ, et al. Hypoxia triggers hedgehog-mediated tumor-stromal interactions in pancreatic cancer. *Cancer research*. 2013; 73:3235–47. [PubMed: 23633488]
5. Chew CS, Chen X, Parente JA Jr, Tarrer S, Okamoto C, Qin HY. Lasp-1 binds to non-muscle F-actin *in vitro* and is localized within multiple sites of dynamic actin assembly *in vivo*. *Journal of cell science*. 2002; 115:4787–99. [PubMed: 12432067]
6. Tomasetto C, Moog-Lutz C, Regnier CH, Schreiber V, Basset P, Rio MC. Lasp-1 (MLN 50) defines a new LIM protein subfamily characterized by the association of LIM and SH3 domains. *FEBS letters*. 1995; 373:245–9. [PubMed: 7589475]
7. Tomasetto C, Regnier C, Moog-Lutz C, Mattei MG, Chenard MP, Lidereau R, et al. Identification of four novel human genes amplified and overexpressed in breast carcinoma and localized to the q11-q21.3 region of chromosome 17. *Genomics*. 1995; 28:367–76. [PubMed: 7490069]
8. Schreiber V, Moog-Lutz C, Regnier CH, Chenard MP, Boeuf H, Vonesch JL, et al. Lasp-1, a novel type of actin-binding protein accumulating in cell membrane extensions. *Molecular medicine*. 1998; 4:675–87. [PubMed: 9848085]
9. Keicher C, Gambaryan S, Schulze E, Marcus K, Meyer HE, Butt E. Phosphorylation of mouse LASP-1 on threonine 156 by cAMP- and cGMP-dependent protein kinase. *Biochemical and biophysical research communications*. 2004; 324:308–16. [PubMed: 15465019]
10. Traenka C, Remke M, Korshunov A, Bender S, Hielscher T, Northcott PA, et al. Role of LIM and SH3 protein 1 (LASP1) in the metastatic dissemination of medulloblastoma. *Cancer research*. 2010; 70:8003–14. [PubMed: 20924110]
11. Rachlin AS, Otey CA. Identification of palladin isoforms and characterization of an isoform-specific interaction between Lasp-1 and palladin. *Journal of cell science*. 2006; 119:995–1004. [PubMed: 16492705]
12. Grunewald TG, Butt E. The LIM and SH3 domain protein family: structural proteins or signal transducers or both? *Molecular cancer*. 2008; 7:31. [PubMed: 18419822]

13. Grunewald TG, Kammerer U, Schulze E, Schindler D, Honig A, Zimmer M, et al. Silencing of LASP-1 influences zyxin localization, inhibits proliferation and reduces migration in breast cancer cells. *Experimental cell research*. 2006; 312:974–82. [PubMed: 16430883]
14. Grunewald TG, Kammerer U, Winkler C, Schindler D, Sickmann A, Honig A, et al. Overexpression of LASP-1 mediates migration and proliferation of human ovarian cancer cells and influences zyxin localisation. *British journal of cancer*. 2007; 96:296–305. [PubMed: 17211471]
15. Zhao L, Wang H, Liu C, Liu Y, Wang X, Wang S, et al. Promotion of colorectal cancer growth and metastasis by the LIM and SH3 domain protein 1. *Gut*. 2010; 59:1226–35. [PubMed: 20660701]
16. Wang B, Feng P, Xiao Z, Ren EC. LIM and SH3 protein 1 (Lasp1) is a novel p53 transcriptional target involved in hepatocellular carcinoma. *J Hepatol*. 2009; 50:528–37. [PubMed: 19155088]
17. Han ZB, Ren H, Zhao H, Chi Y, Chen K, Zhou B, et al. Hypoxia-inducible factor (HIF)-1 alpha directly enhances the transcriptional activity of stem cell factor (SCF) in response to hypoxia and epidermal growth factor (EGF). *Carcinogenesis*. 2008; 29:1853–61. [PubMed: 18339685]
18. Zhao T, Gao S, Wang X, Liu J, Duan Y, Yuan Z, et al. Hypoxia-inducible factor-1alpha regulates chemotactic migration of pancreatic ductal adenocarcinoma cells through directly transactivating the CX3CR1 gene. *PLoS one*. 2012; 7:e43399. [PubMed: 22952674]
19. Yang S, Zhang JJ, Huang XY. Mouse models for tumor metastasis. *Methods in molecular biology*. 2012; 928:221–8. [PubMed: 22956145]
20. Yang S, Huang XY. Ca<sup>2+</sup> influx through L-type Ca<sup>2+</sup> channels controls the trailing tail contraction in growth factor-induced fibroblast cell migration. *The Journal of biological chemistry*. 2005; 280:27130–7. [PubMed: 15911622]
21. Chaturvedi P, Gilkes DM, Wong CC, Kshitiz, Luo W, Zhang H, et al. Hypoxia-inducible factor-dependent breast cancer-mesenchymal stem cell bidirectional signaling promotes metastasis. *The Journal of clinical investigation*. 2013; 123:189–205. [PubMed: 23318994]
22. Fujisawa T, Joshi B, Nakajima A, Puri RK. A novel role of interleukin-13 receptor alpha2 in pancreatic cancer invasion and metastasis. *Cancer research*. 2009; 69:8678–85. [PubMed: 19887609]
23. Zhao X, Gao S, Ren H, Sun W, Zhang H, Sun J, et al. Hypoxia-inducible factor-1 promotes pancreatic ductal adenocarcinoma invasion and metastasis by activating transcription of the actin-bundling protein fascin. *Cancer research*. 2014; 74:2455–64. [PubMed: 24599125]
24. Zhang H, Wong CC, Wei H, Gilkes DM, Korangath P, Chaturvedi P, et al. HIF-1-dependent expression of angiopoietin-like 4 and L1CAM mediates vascular metastasis of hypoxic breast cancer cells to the lungs. *Oncogene*. 2012; 31:1757–70. [PubMed: 21860410]
25. Wong CC, Zhang H, Gilkes DM, Chen J, Wei H, Chaturvedi P, et al. Inhibitors of hypoxia-inducible factor 1 block breast cancer metastatic niche formation and lung metastasis. *Journal of molecular medicine*. 2012; 90:803–15. [PubMed: 22231744]
26. Wang H, Li W, Jin X, Cui S, Zhao L. LIM and SH3 protein 1, a promoter of cell proliferation and migration, is a novel independent prognostic indicator in hepatocellular carcinoma. *Eur J Cancer*. 2013; 49:974–83. [PubMed: 23084841]
27. Yang Y, Sun M, Wang L, Jiao B. HIFs, angiogenesis, and cancer. *Journal of cellular biochemistry*. 2013; 114:967–74. [PubMed: 23225225]
28. Akakura N, Kobayashi M, Horiuchi I, Suzuki A, Wang J, Chen J, et al. Constitutive expression of hypoxia-inducible factor-1alpha renders pancreatic cancer cells resistant to apoptosis induced by hypoxia and nutrient deprivation. *Cancer research*. 2001; 61:6548–54. [PubMed: 11522653]
29. Sun J, He H, Pillai S, Xiong Y, Challa S, Xu L, et al. GATA3 transcription factor abrogates Smad4 transcription factor-mediated fascin overexpression, invadopodium formation, and breast cancer cell invasion. *The Journal of biological chemistry*. 2013; 288:36971–82. [PubMed: 24235142]
30. Sun J, He H, Xiong Y, Lu S, Shen J, Cheng A, et al. Fascin protein is critical for transforming growth factor beta protein-induced invasion and filopodia formation in spindle-shaped tumor cells. *The Journal of biological chemistry*. 2011; 286:38865–75. [PubMed: 21914811]
31. Chen L, Yang S, Jakoncic J, Zhang JJ, Huang XY. Migrastatin analogues target fascin to block tumour metastasis. *Nature*. 2010; 464:1062–6. [PubMed: 20393565]

32. Yang S, Huang FK, Huang J, Chen S, Jakoncic J, Leo-Macias A, et al. Molecular mechanism of fascin function in filopodial formation. *The Journal of biological chemistry*. 2013; 288:274–84. [PubMed: 23184945]
33. Ostapoff KT, Kutluk Cenik B, Wang M, Ye R, Xu X, Nugent D, et al. Neutralizing murine TGFbetaR2 promotes a differentiated tumor cell phenotype and inhibits pancreatic cancer metastasis. *Cancer research*. 2014
34. Gohrig A, Detjen KM, Hilfenhaus G, Korner JL, Welzel M, Arsenic R, et al. Axon guidance factor SLIT2 inhibits neural invasion and metastasis in pancreatic cancer. *Cancer research*. 2014; 74:1529–40. [PubMed: 24448236]
35. Singh AP, Arora S, Bhardwaj A, Srivastava SK, Kadakia MP, Wang B, et al. CXCL12/CXCR4 protein signaling axis induces sonic hedgehog expression in pancreatic cancer cells via extracellular regulated kinase- and Akt kinase-mediated activation of nuclear factor kappaB: implications for bidirectional tumor-stromal interactions. *The Journal of biological chemistry*. 2012; 287:39115–24. [PubMed: 22995914]

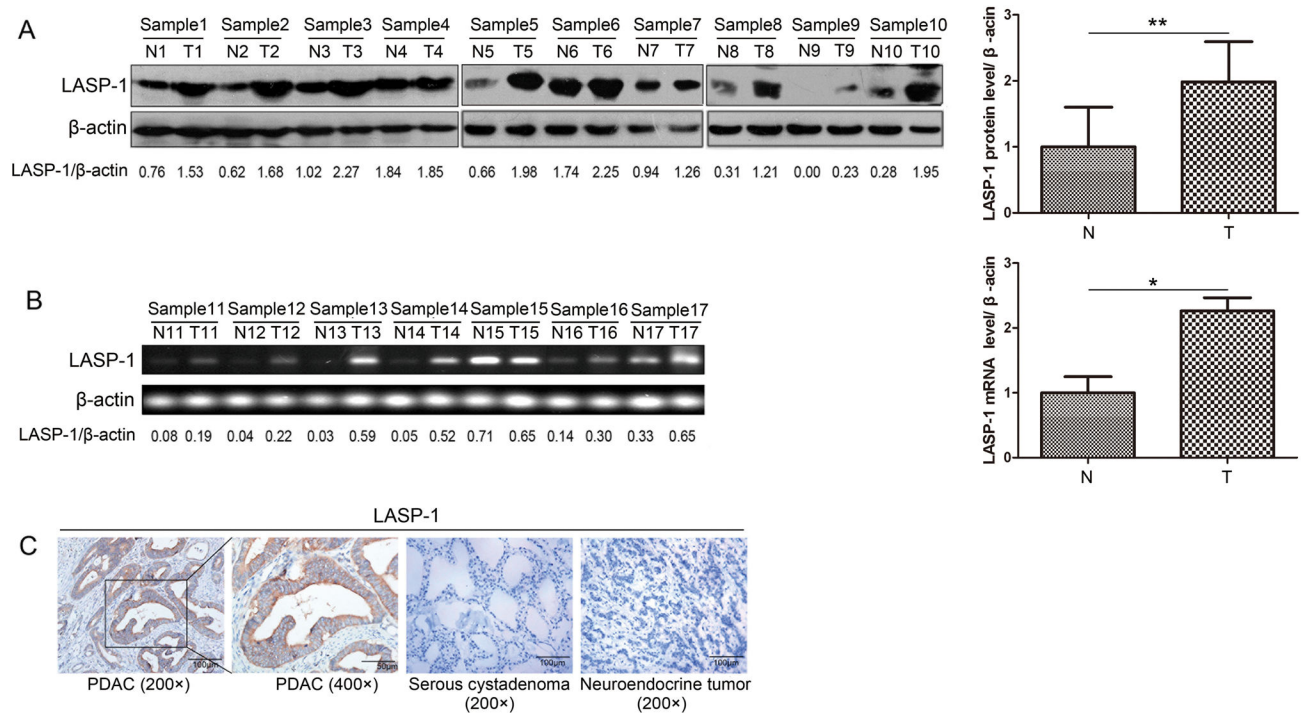


**Figure 1. LASP-1 is overexpressed in the specimens of PDAC**

(A) Left: Western blot analysis of LASP-1 levels in ten total paired human PDAC tumorous and matched adjacent non-tumorous tissues. LASP-1 protein expression levels were normalized by those of β-actin. Right: The chart showed that LASP-1 protein expression levels in PDAC specimens versus paired adjacent normal pancreatic tissues. (N: Normal; T: Tumor),  $**p < 0.01$ . (B) Left: RT-PCR analysis of LASP-1 levels in seven total paired human PDAC tumorous and matched adjacent non-tumorous tissues. LASP-1 mRNA expression levels were normalized by β-actin. Right: The chart showed that LASP-1 mRNA expression levels in PDAC specimens versus paired adjacent normal pancreatic tissues. (N: Normal; T: Tumor),  $*p < 0.05$ . (C) Expression analysis of LASP-1 protein in PDAC, serous cystadenoma and neuroendocrine tumor tissues by immunohistochemistry. (magnification, 200× or 400×).

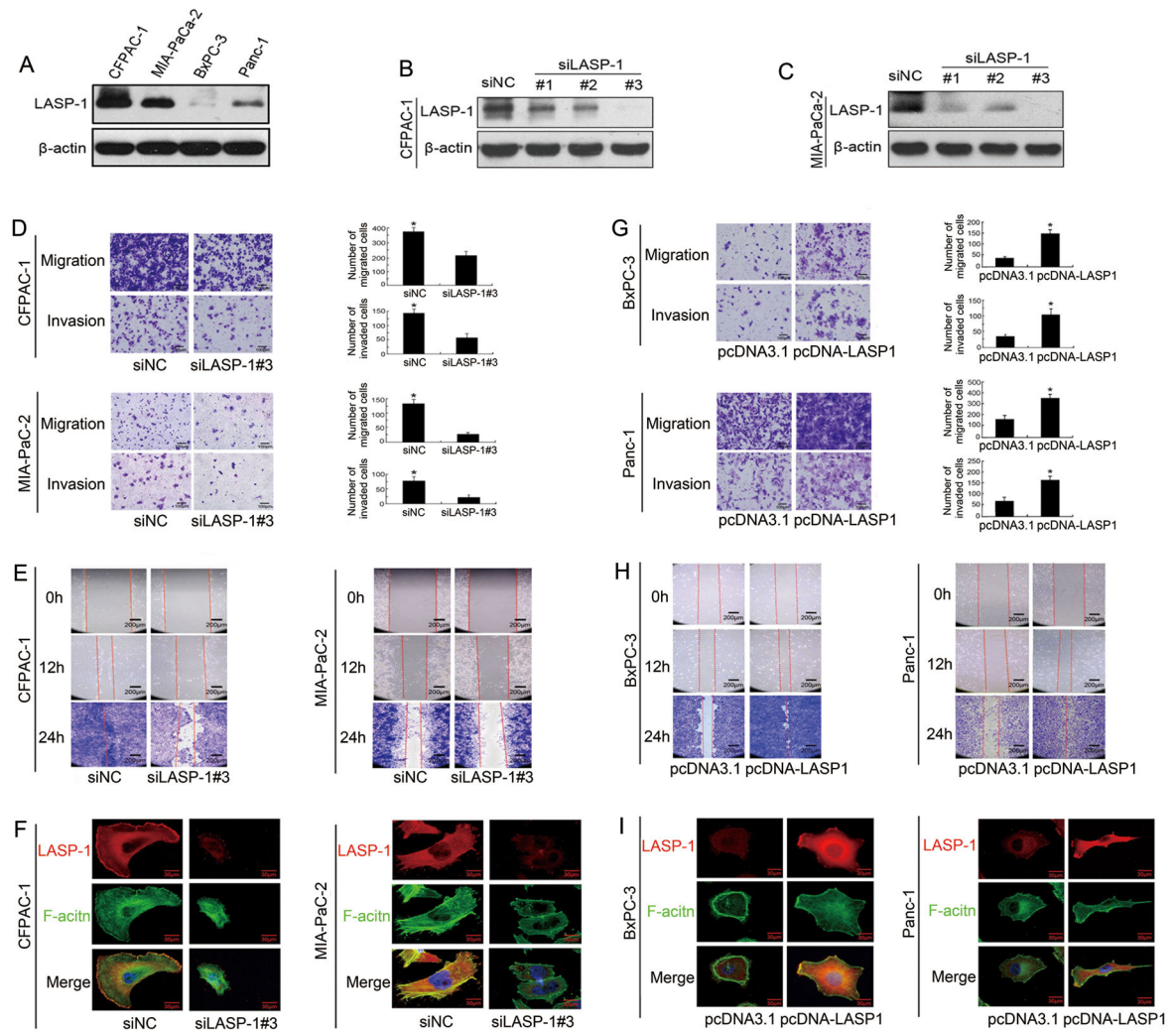


**Figure 2. LASP-1 promotes PDAC cell migration and invasion**

(A) The basic expression of LASP-1 protein in four human PDAC cells was assessed by Western blot experiment. (B, C) LASP-1 protein expression in CFPAC-1 and MIA-PaCa2 cells transfected with negative control siRNA (siNC) and LASP-1 siRNA (siLASP-1#1-3) (50 nM) for 48 hours was determined by Western blot.  $\beta$ -actin was used as a loading control. (D) Comparison of migration and invasion potential of CFPAC-1 (upper) and MIA-PaCa2 (lower) cells transfected with negative control (NC) siRNA and LASP-1 siRNA#3 (50 nM) for 48 hours using Boyden chambers. The experiments were performed independently for three times. \* $p < 0.05$  versus control. (magnification, 200 $\times$ ). (E) Wound-healing assays comparing the motility of CFPAC-1 (left) and MIA-PaCa2 (right) cells transfected with NC siRNA and LASP-1 siRNA#3 (50 nM) for 48 hours. (magnification, 100 $\times$ ). (F) Confocal images of CFPAC-1 (left) and MIA-PaCa2 (right) cells transfected with NC siRNA and LASP-1 siRNA#3 (50 nM) stained for LASP-1 (red), F-actin (green), and 4',6-diamidino-2-phenylindole (DAPI; blue) (magnification, 600 $\times$ ). Co-localization was indicated by the merged images showing yellow immunofluorescence. (G) Comparison of the migration and invasion potential of BxPC-3 (upper) and Panc-1 (lower) cells transfected with pcDNA3.1

and pcDNA3.1-LASP1 plasmids (2  $\mu$ g) for 48 hours using Boyden chambers. The experiments were performed independently for three times. \* $p < 0.05$  versus control. (magnification, 200 $\times$ ). (H) Wound-healing assays comparing the migration of BxPC-3 (left) and Panc-1 (right) cells transfected with pcDNA3.1 and pcDNA3.1-LASP1 plasmids (2  $\mu$ g) for 48 hours. (magnification, 100 $\times$ ). (I) Confocal images of BxPC-3 (left) and Panc-1 (right) cells transfected with pcDNA3.1 and pcDNA3.1-LASP1 plasmids (2  $\mu$ g) stained for F-actin (red) and 4',6-diamidino-2-phenylindole (DAPI; blue) (magnification, 600 $\times$ ). Co-localization was indicated by the merged images showing yellow immunofluorescence.

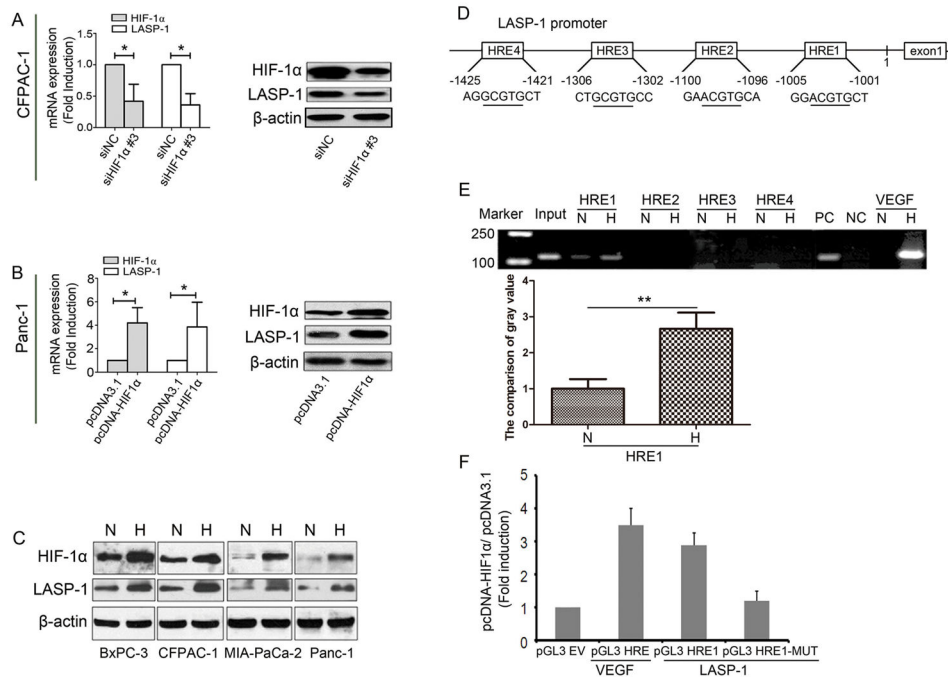


**Figure 3. LASP-1 is a novel HIF-1α target gene critical for HIF-1α induced cell migration** (A) CFPAC-1 cells were transfected with siHIF-1α #3 (50 nM) for 48 h and assessed HIF-1α and LASP-1 expression by qRT-PCR (left) and Western blot (right) analysis. The experiments were performed independently for three times. \* $p < 0.05$  versus control. (B) Panc-1 cells were transfected with pcDNA3.1-HIF1α plasmids (2 μg) for 48 hours and assessed HIF-1α and LASP-1 expression by qRT-PCR (left) and Western blot (right) analysis. The experiments were performed independently for three times. \* $p < 0.05$  versus control. (C) HIF-1α and LASP-1 expression determined by Western blot analysis on four human PDAC cells cultured under normoxia (21% O<sub>2</sub>) and hypoxia (1.5% O<sub>2</sub>) for 12 hours. (N: Normoxia; H: Hypoxia). (D) The DNA sequence of the LASP-1 promoter. Four HRE sites are located at the different site. (E) Upper: Chromatin immunoprecipitation analysis HIF-1 binding to LASP-1 promoter in Panc-1 cells. The PCR products of VEGF promoter were used as positive control. H, N, PC and NC indicate hypoxia, normoxia, positive control and negative control, respectively. Lower: The comparison of gray value between normoxia and hypoxia in HRE1. \*\* $p < 0.01$ . The experiments were performed independently for three times. (F) Luciferase analysis in Panc-1 cells. Panc-1 cells overexpressing HIF-1α expression plasmids (pcDNA-HIF1α) or control vector (pcDNA3.1) were transfected with pGL3-LASP-1-promoter, pGL3-LASP-1-promoter-mutation, pGL3-VEGF-promoter, or pGL3-empty vector. After transfection for 48 hours, cells were subjected to dual luciferase analysis. Results were expressed as a fold induction relative to the cells transfected with the control vector (pcDNA3.1) after normalization to Renilla activity. The experiments were performed independently for three times.

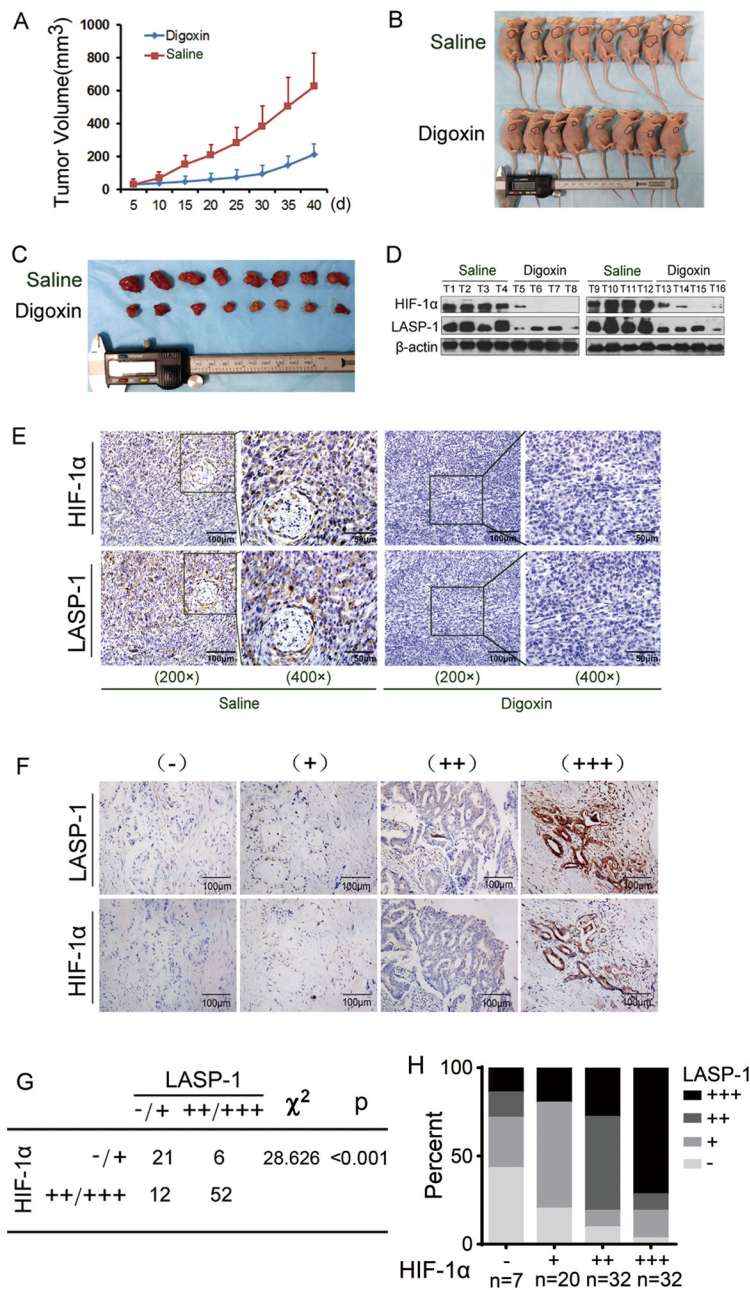


**Figure 4. HIF-1α promotes LASP-1 overexpression in xenograft PDAC mouse model and PDAC patients specimens**  
 (A) Panc-1 cells were subcutaneously implanted into the nude nu/nu mice, which were treated with saline or digoxin (2 mg/kg) everyday. The data of all primary tumors are expressed as mean ± SD. (B) Representative images of mice injected with Panc-1 cells subcutaneously implanted into the nude mice (nu/nu). (C) Representative figure of tumors formed. (D) HIF-1α and LASP-1 expression determined by Western blot analysis in pancreatic cancer tissues of nude mice (nu/nu) treated by saline or digoxin. (E) Representative immunohistochemical staining of HIF-1α and LASP-1 in pancreatic cancer tissues of nude nu/nu mice treated by saline or digoxin. (magnification, 200× and 400×). (F)



Immunohistochemical analysis of HIF-1 $\alpha$  and LASP-1 correlative expression in human PDAC surgical samples. (magnification, 200 $\times$ ). (G) Statistical analysis of immunohistochemical results of HIF-1 $\alpha$  and LASP-1 expression in human PDAC surgical samples. *p* values were analyzed by Chi-Square test. (F) The real distribution of immunohistochemical results between HIF-1 $\alpha$  and LASP-1 expression.

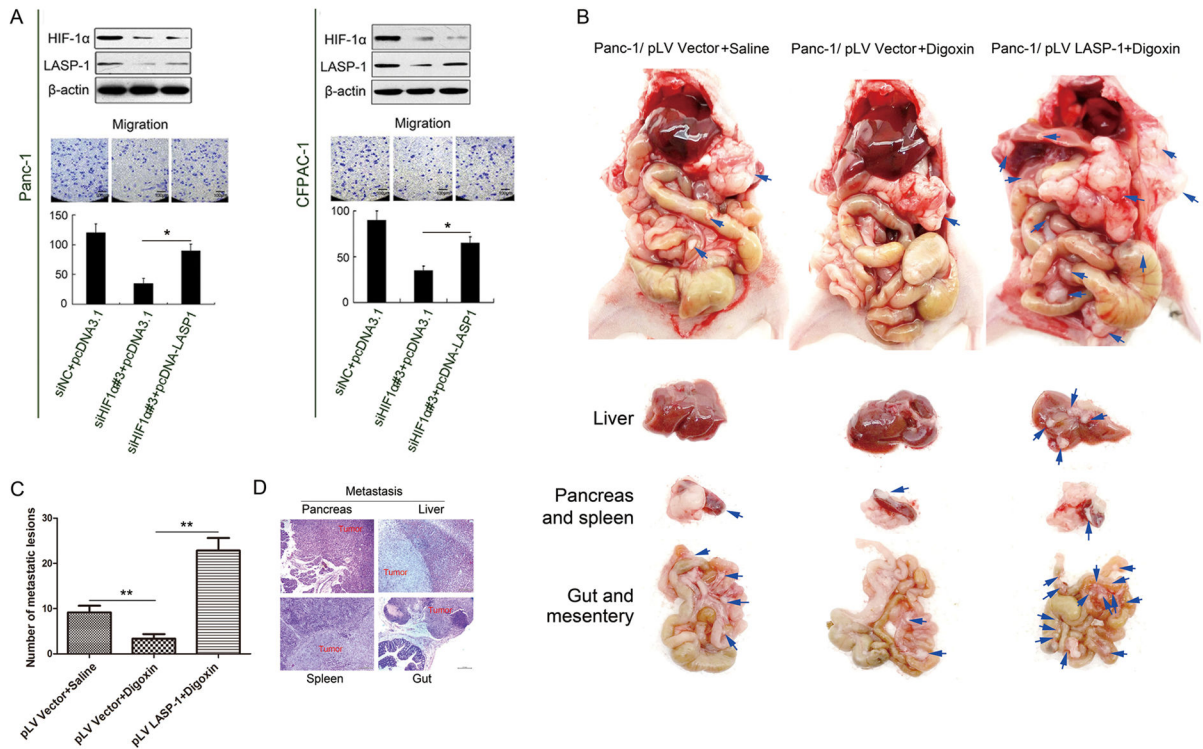


**Figure 5. LASP-1 is critical for PDAC metastasis in a orthotopic mouse model**

(A) Panc-1(left) and CFPAC-1(right) cells were co-transfected with siHIF1α(50 nM) and pcDNA3.1-LASP-1 (2 μg) plasmids and assessed by Western blot (upper) and Boyden chambers. (lower) analysis. The experiments were performed independently for three times. \* $p < 0.05$ . (magnification, 200×). (B) The orthotopic xenograft pancreatic cancer mouse model using Panc-1/pLV Vector and Panc-1/pLV LASP-1 cells were treated with saline or digoxin. Representative images of primary pancreatic tumor and metastatic tumors of liver, gut and mesentery were shown. (C) Statistical analysis of the total number of visible metastatic lesions in liver, gut and mesentery by t-test. Data were presented as mean±SD. \*\* $p < 0.01$ . (D) Hematoxylin-eosin staining verified the tumors from pancreas, liver, gut and spleen. (magnification, 100×).

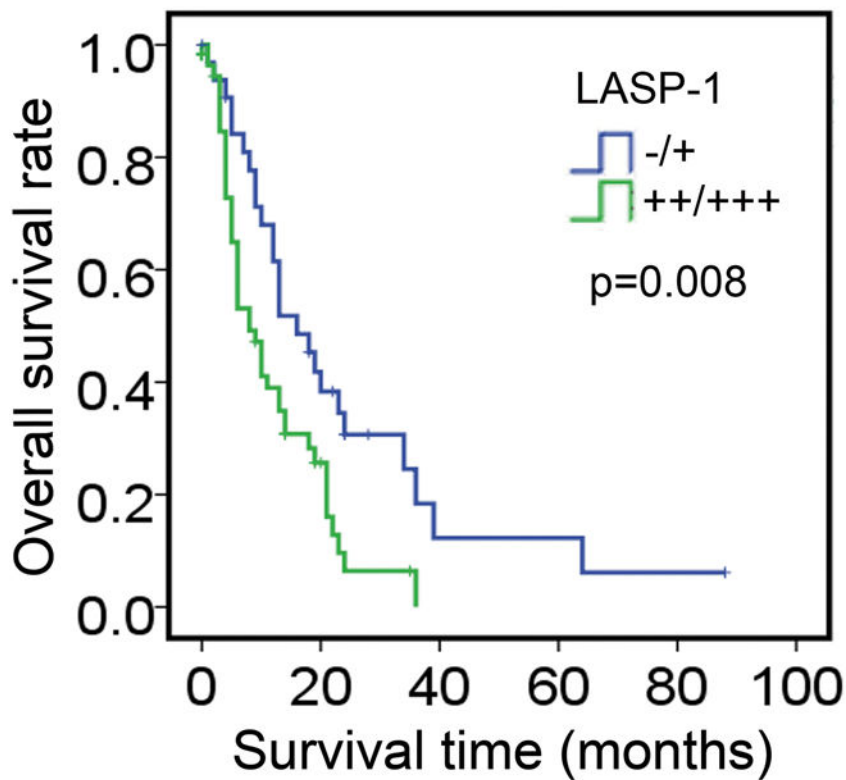


**Figure 6. LASP-1 influences the prognosis of PDAC patients**

Association between LASP-1 expression levels and the overall survival of PDAC patients. PDAC patients (n=91) were stratified into two groups according to LASP-1 IHC staining intensity. Patients with high LASP-1 expression (intensity grade ++ and +++) had much worse overall survival when compared to patients with low LASP-1 expression (intensity grade – and +).  $p=0.008$  was determined with the Log-rank test.

**Table 1**

Correlation of LASP-1 expression to clinicopathological features in PDAC

Parameters	LASP-1				$\chi^2$	p
	-	+	++	+++		
Age (years)					1.147	0.766
60	6	10	12	23		
>60	5	12	9	14		
Gender					1.913	0.591
Male	5	15	13	21		
Female	6	7	8	16		
pTNM stage					21.806	0.010*
I	1	5	0	0		
II	6	13	13	15		
III	2	4	5	12		
IV	2	0	3	10		
Histological grade					5.023	0.541
G1	5	9	4	14		
G2	3	5	9	8		
G3	3	8	8	15		
LN metastasis					17.481	0.001*
N0	5	16	11	7		
N1	6	6	10	30		

Statistical data of LASP-1 expression in relation to clinicopathological features in PDAC surgical samples. Values of p were calculated by Chi-Square test. N0 and N1 refer to the absence and presence of regional lymph node (LN) metastasis, respectively. pTNM stage refers to the pathological tumor node metastasis (pTNM) stage.

\* Statistically significant ( $p < 0.05$ ).